Journal of Applied Mechanics and Technical Physics, Vol. 47, No. 6, pp. 911–917, 2006

ANALYSIS OF REINFORCED-CONCRETE STRENGTH UNDER IMPACT LOADING

N. N. Belov,[1] O. V. Kabantsev,[2] A. A. Konyaev,[3] D. G. Kopanitsa,[1] V. F. Tolkachev,[3] A. A. Yugov,[1] and N. T. Yugov[4]

UDC 539.3

A mathematical model is proposed to describe deformation and fracture of reinforced concrete under impact loading within the framework of mechanics of continuous media. The problem of the impact of steel cylindrical projectiles on rectangular slabs made of reinforced concrete is solved. The results of mathematical modeling are in good agreement with experimental data.

Key words: *impact, fracture, concrete, reinforced concrete, mathematical modeling.*

The problem of impact interaction of cylindrical projectiles with rectangular concrete and reinforced-concrete slabs was solved in [1–3]. Concrete fracture was calculated by a phenomenological approach where the strength criteria are expressed in terms of invariant relations between the critical values of macrocharacteristics of the process (stresses and strains). Until the failure criterion is reached, the concrete behavior under dynamic loading is described by the model of a linear elastic body possessing physical and mechanical properties of concrete. As the failure criterion is satisfied, the material is assumed to be damaged by cracks. Fragmentation of the damaged material is described within the framework of the model of a porous elastoplastic medium. Fragmentation of the crack-damaged material subjected to tensile stresses occurs when the relative volume of voids reaches a critical value. If the crack-damaged material is subjected to compressive stresses, the local criterion of fragmentation is either the limiting value of the work of plastic strains or the limiting value of intensity of plastic strains, which is uniquely related to the first factor. The fractured material behaves as a granulated medium that can withstand compressive and shear stresses but fails under the action of tensile stresses. The results of mathematical modeling of impact interaction of steel cylindrical elements with concrete slabs compared with experimental data showed that this approach can be used to calculate the strength of elements of reinforced-concrete structures under dynamic loading.

In calculating reinforced-concrete structures, the concrete layer with reinforcing bars is modeled by an elastoplastic medium, which is a homogeneous two-phase mixture of steel and concrete. In contrast to concrete whose typical feature is brittle fracture, the fracture of the homogeneous two-phase mixture of steel and concrete is rather similar to that of plastic materials [4].

A mathematical model that allows calculating deformation and fracture of high-strength porous ceramics under explosive and impact loading within the framework of mechanics of continuous media was developed in [5–7]. An advantage of this model is the possibility of studying the fracture in porous ceramics under multiple impact loading. This mathematical model was used in [8] to study the mechanisms of particle refinement for obtaining submicron powders in a pneumatic circular machine. This model can be readily adapted to calculating the strength of foam concrete under dynamic loading.

[1]Tomsk State University of Architecture and Building, Tomsk 634003; YugAlex@mail.ru. [2]Central Design Institute No. 53, Ministry of Defense of the Russian Federation, Moscow 125252. [3]Institute of Applied Mathematics and Mechanics at the Tomsk State University, Tomsk 634050. [4]Tomsk State University of Control Systems and Radioelectronics, Tomsk 634050; . Translated from Prikladnaya Mekhanika i Tekhnicheskaya Fizika, Vol. 47, No. 6, pp. 165–173, November–December, 2006. Original article submitted October 19, 2005.

The model of dynamic deformation and fracture of high-strength porous ceramics was used in the present work to calculate the strength of rectangular reinforced-concrete slabs under impact interaction with cylindrical steel projectiles. The results obtained were compared with the results of calculations within the framework of the phenomenological approach and with experimental data.

1. Mathematical Model. Concrete contains a large number of stress concentrators: pores, grain boundaries, or cracks, where the fracture originates in the region of elastic strains. Microfracture in concrete can appear owing to compression under the action of deviatoric stresses, which reduces concrete resistance to fracture.

An inhomogeneous porous medium is a two-species material consisting of a solid phase (matrix) and inclusions (pores). The pores are assumed to have a more or less spherical shape, and their size distribution function is such that the entire ensemble of pores can be characterized by a certain characteristic size a_0. The specific volume of the porous medium v is presented as the sum of the specific volume of the matrix material v_m, specific volume of the pores v_p, and specific volume occupied by the crack v_t ($v = v_m + v_p + v_t$). The material porosity is characterized by the dimensionless volume of voids $\xi = \xi_p + \xi_t$ ($\xi_p = v_p/v$ and $\xi_t = v_t/v$ are the dimensionless volumes of pores and cracks, respectively [1, 5–7]) or by the parameter $\alpha = v/v_m$. These quantities are related as $\alpha = 1/(1-\xi)$.

The system of equations that describe the motion of a porous elastoplastic medium has the form

$$\frac{d}{dt}\int\limits_V \rho\,dV = 0, \qquad \frac{d}{dt}\int\limits_V \rho\boldsymbol{u}\,dV = \int\limits_S \boldsymbol{n}\cdot\sigma\,dS, \qquad \frac{d}{dt}\int\limits_V \rho E\,dV = \int\limits_S \boldsymbol{n}\cdot\sigma\cdot\boldsymbol{u}\,dS,$$

$$e = \frac{s^J}{2\mu} + \lambda s, \qquad s : s = \frac{2}{3}\,\sigma_{\text{yield}}^2, \qquad p = \frac{\rho_0}{\alpha}\Big(\gamma_0\varepsilon + \frac{c_0^2(1-\gamma_0\eta/2)\eta}{(1-S_0\eta)^2}\Big), \tag{1.1}$$

where t is the time, V is the domain of integration, S is the surface bounding the domain of integration, $\boldsymbol{n}$ is the unit vector of the external normal, ρ is the density, $\sigma = -pg + s$ is the stress tensor, s is the deviator, p is the pressure, $\boldsymbol{u}$ is the velocity vector, $E = \varepsilon + \boldsymbol{u}\cdot\boldsymbol{u}/2$ is the specific total energy, ε is the specific internal energy, $e = d - (d:g)g/3$ is the deviator of the strain-rate tensor, g is the metric tensor, $d = (\nabla\boldsymbol{u} + \nabla\boldsymbol{u}R^{\text{t}})/2$ is the strain-rate tensor, $s^J = \dot{s} + s\omega - \omega s$ is the Jaumann–Noll derivative of the stress deviator, $\mu = \mu_0(1-\xi)[1-(6\rho_0c_0^2+12\mu_0)\xi/(9\rho_0c_0^2+8\mu_0)]$ is the shear modulus, $\sigma_{\text{yield}} = \{\sigma_{\min} + (\sigma_{\max}-\sigma_{\min})kp/[(\sigma_{\max}-\sigma_{\min}) + kp]\}/\alpha$ is the yield strength, $\omega = (\nabla u^{\text{t}} - \nabla u)/2$ is the vorticity tensor, ρ_0, c_0, μ_0, $\sigma_{\min}$, $\sigma_{\max}$, k, S_0, and γ_0 are constants of the matrix material, and $\eta = 1 - \rho_0 v/\alpha$. The parameter λ is eliminated by using the yield condition.

To close system (1.1), we need equations that describe the change in the parameter α under extension and compression. Fracture of brittle materials mainly occurs owing to origination and growth of microcracks. The maximum elastic half-opening of a coin-shaped crack under the action of tensile stresses perpendicular to the crack plane is determined by the relation [9]

$$\delta = -\frac{2(1-\nu)}{\pi\mu_0}\,Rp_m,$$

where ν is Poisson's ratio, R is the crack radius, and $p_m = \alpha p$ is the pressure in the matrix material. Assuming that the crack edges form an ellipsoid of revolution with semiaxes δ, R, and R during crack opening, we can find the crack volume

$$V_t = -\frac{8(1-\nu)}{3\mu_0}\,R^3\alpha p. \tag{1.2}$$

Let no new cracks be formed during loading, but material deformation involve the growth of initially existing cracks with the characteristic size R. Then Eq. (1.2) gives

$$\xi_t = -\frac{8(1-\nu)}{3\mu_0}\,N_0R^3\alpha p, \tag{1.3}$$

where N_0 is the number of cracks in a unit volume. Assuming that the volume of pores remains unchanged before the beginning of fragmentation of the material damaged by cracks and is equal to ξ_0, we obtain

$$\xi_t = \xi - \xi_0 = \frac{\alpha - \alpha_0}{\alpha_0\alpha}. \tag{1.4}$$

Substituting Eq. (1.4) into Eq. (1.3), we finally obtain

$$p = -\frac{3\mu_0(\alpha - \alpha_0)}{8(1-\nu)N_0\alpha_0 R^3\alpha^2}. \tag{1.5}$$

It follows from Eq. (1.5) that the mean pressure decreases with increasing crack radius. The crack growth is described by the equation

$$\dot{R}/R = F_1 + F_2.$$

Here $F_1 = (\alpha s_i - s_*)/\eta_1$ for $\alpha s_i > s_*$ and $F_1 = 0$ for $\alpha s_i \leqslant s_*$, $F_2 = (|\alpha p| - p_*)/\eta_2$ for $p < 0$ and $|\alpha p| > p_*$ and $F_2 = 0$ for $p \geqslant 0$ or $|\alpha p| \leqslant p_*$; $s_i = \sqrt{(3/2)s : s}$, $s_* = s_{01}(1 - R/R_*)$, $p_* = p_0(1 - R/R_*)$, and $R_* = \beta/\sqrt[3]{N_0}$, s_{01}, p_0, η_1, η_2, and β are constants of the material.

Coalescence of microcracks in sufficiently plastic materials occurs when they come into contact. The calculations of the system of elastic cracks show that their interaction and coalescence occur if the distance between the ends of the neighboring cracks is two or three crack sizes [10]. The critical distance depends on the size of the zone around the crack where the stress concentration is rather significant. Constructing a model that could quantify the coalescence of microdefects up to formation of microscopic fragments is a complicated problem. It is assumed that the cracks start to merge when their characteristic size R with a constant number of cracks in a unit volume N_0 reaches a critical value $R_* = \beta/\sqrt[3]{N_0}$. The fragmentation of the crack-damaged material and the behavior of the fractured material are described by the model of a porous elastoplastic medium. System (1.1) is closed by the following equations relating the pressure p and porosity α:

— under compression $[p \geqslant (2/3)\sigma_{\text{yield}} \ln(\alpha/(\alpha - 1))]$,

$$\left(\gamma_0\varepsilon\rho_0 + \frac{\rho_0 c_0^2(1 - \gamma_0\eta/2)\eta}{(1 - S_0\eta)^2}\right) - \frac{2}{3}\,\sigma_{\text{yield}} \ln\frac{\alpha}{\alpha - 1} = 0;$$

— under unloading $[p \leqslant -a_S \ln(\alpha/(\alpha - 1))]$,

$$\left(\gamma_0\varepsilon\rho_0 + \frac{\rho_0 c_0^2(1 - \gamma_0\eta/2)\eta}{(1 - S_0\eta)^2}\right) + a_S \ln\,\frac{\alpha}{\alpha - 1} = 0.$$

Fragmentation of the crack-damaged material subjected to tensile stresses occurs when the relative volume of voids reaches the critical value $\xi_* = (\alpha_* - 1)/\alpha_*$. If the crack-damaged material is subjected to compressive stresses, the fragmentation criterion is the limiting intensity of plastic strains

$$e_u = (\sqrt{2}/3)\sqrt{3T_2 - T_1^2}$$

(T_1 and T_2 are the first and second invariants of the strain tensor, respectively). Under extension, the fragmented material is modeled as a powder whose motion obeys the equations of the medium in the absence of stresses [2].

In calculating reinforced-concrete slabs, the layer of concrete with reinforcing bars is modeled by an elastoplastic medium [1[, which is a homogeneous two-phase mixture of steel and concrete whose initial density $\rho_{0,\text{rc}}$ is determined by the formula

$$\rho_{0,\text{rc}} = \nu_1\rho_{0,\text{s}} + \nu_2\rho_{0,\text{c}},$$

where ν_1, ν_2 and $\rho_{0,\text{s}}$, $\rho_{0,\text{c}}$ are the initial volume concentrations and densities of steel and concrete , respectively ($\nu_1 + \nu_2 = 1$). The volume concentrations are determined via the areas occupied by steel and concrete in a cross section perpendicular to the direction of the reinforcing bar:

$$\nu_1 = \pi d_1 n/(4L), \qquad \nu_2 = 1 - \nu_1.$$

Here L is the bar length, n is the number of bars in a band of length L, and d_1 is the bar diameter.

The equation of state of the reinforced concrete (mixture) has the form

$$p_m = \frac{\rho_{0,\text{rc}} c_{0S}^2(1 - \gamma_S\eta/2)\eta}{(1 - S_{0S}\eta)^2} + \gamma_S\rho_{0,\text{rc}}\varepsilon,$$

where $\eta = 1 - \rho_{0,\text{rc}}v$ (v is the specific volume of the mixture), γ_S is the Grüneisen coefficient, and $v_{0,\text{rc}} = 1/\rho_{0,\text{rc}}$.

The coefficients c_{0S} and S_{0S} of the linear dependence of the shock-wave velocity D in the mixture on the mass velocity and $D = c_{0S} + S_{0S}u$ are determined from the shock adiabats of the components of the mixture:

$$D_i = c_{0i} + S_{0i}u_i \qquad (i = 1, 2).$$

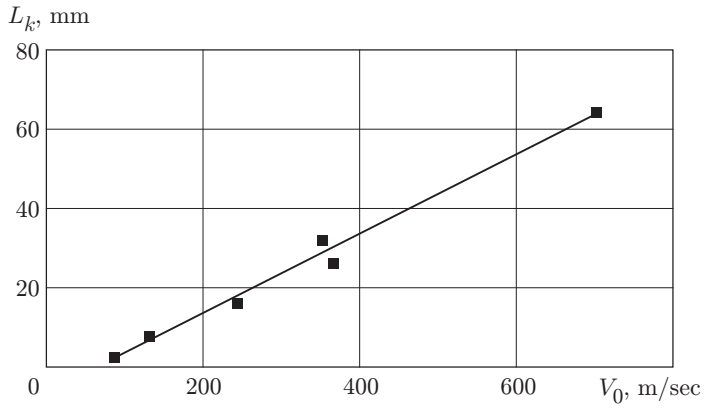

Fig. 1. Penetration depth L_k versus the impact velocity V_0.

TABLE 1

Type of research	$u_0 = 244$ m/sec		$u_0 = 370$ m/sec	
	L_k, mm	D_k	L_k, mm	D_k
Calculation by the phenomenological model	17.3	$2.4d_0$	24.6	$3.8d_0$
Calculation by the model proposed	16.3	$4.5d_0$	26.6	$6d_0$
Experiment	18.0	—	28.0	$5.3d_0$

The Grüneisen coefficient γ_S for the mixture is determined via the Grüneisen coefficients for the components γ_{0i}:

$$\frac{v_{0,\mathrm{rc}}}{\gamma_S} = \sum_{i=1}^{2} \frac{m_i v_{0i}}{\gamma_{0i}}.$$

The shear modulus of the mixture μ_{0S} and the yield strength $\sigma_{\mathrm{yield},S}$ are determined by the formulas

$$\mu_{0S} = 1/(\nu_1/\mu_{01} + \nu_2/\mu_{02}), \qquad \sigma_{\mathrm{yield},S} = m_1\sigma_{\mathrm{yield},1} + m_2\sigma_{\mathrm{yield},2},$$

where $m_i = \nu_i\rho_{0i}/\rho_{0,\mathrm{rc}}$ are the mass concentrations of steel ($i = 1$) and concrete ($i = 2$) in the reinforced layer of concrete; μ_{0i} and $\sigma_{\mathrm{yield},i}$ ($i = 1, 2$) are the shear moduli and the yield strengths of the components of the mixture, respectively.

2. Calculation Results. The parameters of the model of concrete deformation and fracture under dynamic loads were determined with allowance for experimental data on impact loading of slabs made of fine-grain concrete by steel projectiles with impact velocities of 130–700 m/sec [6]. The projectiles were cylinders 7.6 mm in diameter with a constant mass of 8.1 g. The slab thickness was 200 mm.

The impact occurred at an angle of 90° to the frontal face of the slab. In all cases considered, the projectiles remained almost undeformed during penetration. Figure 1 shows the depth of penetration of projectiles into concrete L_k as a function of the impact velocity V_0. The model parameters were refined on the basis of the penetration depth and diameter of spalling on the frontal face.

The following physical and mechanical characteristics of materials and models were used: for concrete, $\rho_0 = 2.2$ g/cm^3, $\mu_0 = 17$ GPa, $c_0 = 0.233$ cm/μsec, $\gamma_0 = 2$, $S_0 = 1.51$, $\sigma_{\min} = 0.0077$ GPa, $\sigma_{\max} = 0.216$ GPa, $k = 0.82$, $\nu = 0.256$, $R_0 = 2.5$ μm, $R_* = 11.6$ μm, $N_0 = 64 \cdot 10^7$ cm^{-3}, $\eta_1 = 7000$ GPa $\cdot\, \mu$sec, $\eta_2 = 800$ GPa $\cdot\, \mu$sec, $p_0 = 0.009\,24$ GPa, $S_{01} = 0.0924$ GPa, $\beta = 1$, $\alpha_0 = 1.01$, $a_S = 0.042$ GPa, $\xi_* = 0.013$, and $e_u^* = 0.15$; for steel, $\rho_0 = 7.85$ g/cm^3, $\mu_0 = 82$ GPa, $c_0 = 0.457$ cm/μsec, $\gamma_0 = 2$, $S_0 = 1.49$, $\sigma_{\min} = 0.6$ GPa, $\alpha_0 = 1.0006$, $a_S = 0.29$ GPa, $\xi_* = 0.3$, and $e_u^* = 1$.

The calculation results and the experimental data [6] for two impact velocities are summarized in Table 1 (u_0 is the impact velocity, L_k is the crater depth, D_k is the diameter of spalling on the frontal face, and d_0 is the projectile diameter). The experiments were performed on a ballistic testbench of the Institute of Applied Mathematics and Mechanics at the Tomsk State University.

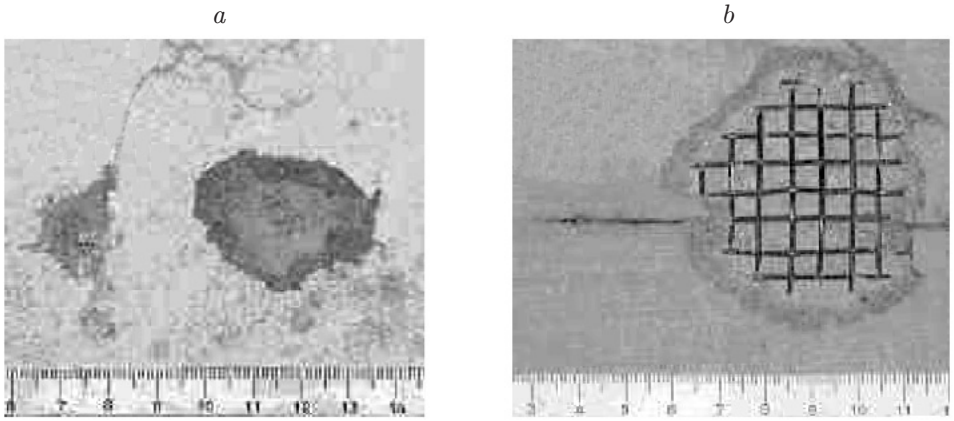

Fig. 2. Photographs of spalling on the frontal face (a) and on the rear face (b) of the reinforced-concrete slab under the impact of a compact projectile with a velocity $u_0 = 462$ m/sec.

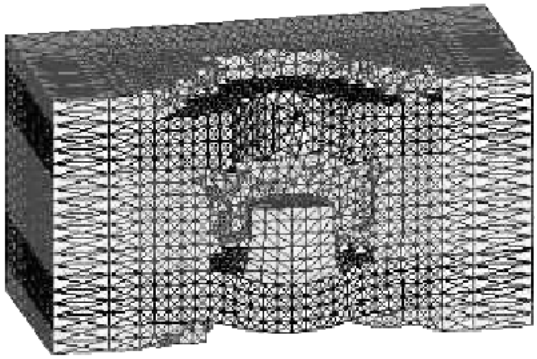

Fig. 3. Fracture of the reinforced-concrete slab under the impact of a compact projectile with a velocity $u_0 = 462$ m/sec.

Both models predict the pattern of interaction of cylindrical projectiles with a concrete slab, which is qualitatively similar to experimental data in terms of the shape of craters, existence of spalling on the frontal face, and insignificant deformation of the projectile. At the same time, there are some differences between the numerical and experimental values of some parameters. For instance, the difference in the crater depth calculated by the phenomenological approach from the experimental value is 4 and 12% for impact velocities $u_0 = 244$ and 370 m/sec, respectively. In calculations by the model proposed here, the difference in L_k for these impact velocities is 9 and 15%. In all cases considered, the predicted crater depth is smaller than that in the experiment. The crater depths predicted by both models differ insignificantly.

The diameters of spalling on the frontal face obtained by calculations and in the experiment differ rather substantially. The maximum diameters of spalling on the frontal face for the above-mentioned impact velocities predicted by the phenomenological approach are $2.4d_0$ and $3.8d_0$, whereas the present model gives $4.5d_0$ and $6d_0$. In the experiment, the diameter of spalling on the frontal face could be measured for the impact velocity $u_0 = 370$ m/sec only. The maximum diameter is $5.3d_0$ and differs from the predicted values by 28 and 13%. With allowance for the data of Isaev [11] who noted that the diameter of frontal spalling in concrete under the impact of projectiles in this range of velocities is $4d_0$–$6d_0$, we can conclude that the results predicted by the present model are in better agreement with available experimental data.

Special experimental investigations were performed for verification of the model of deformation and fracture of reinforced-concrete slabs under impact loading. The concrete slabs 24 and 36 mm thick were reinforced by two layers of a steel net close to the frontal and rear faces. The thickness of steel wire was 1.2 mm, and the cell size was 5×5 mm. The projectile was a compact cylinder (the cylinder height and diameter were identical and equal

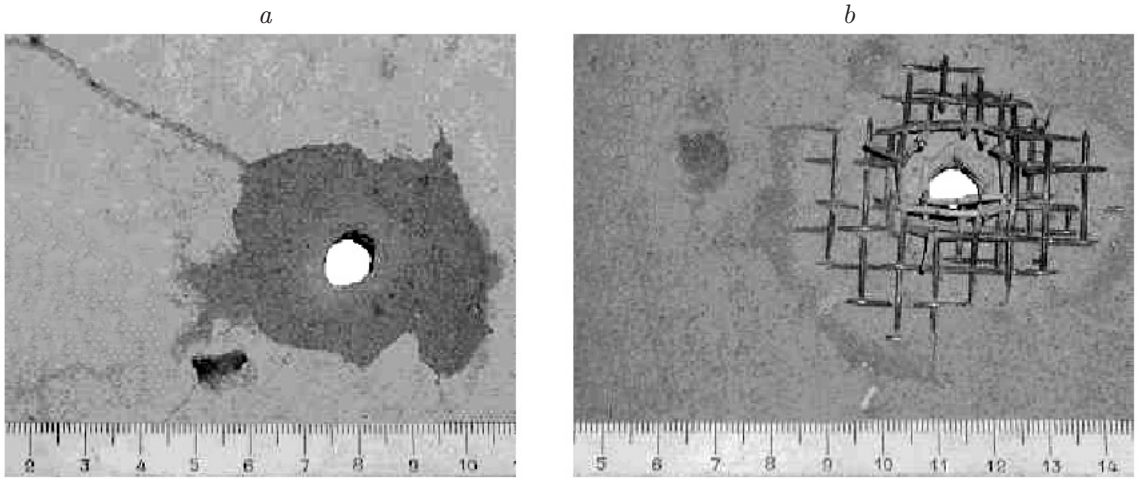

Fig. 4. Photographs of the frontal (a) and rear (b) surfaces of the reinforced-concrete slab under the impact of an extended projectile with a velocity $u_0 = 458$ m/sec.

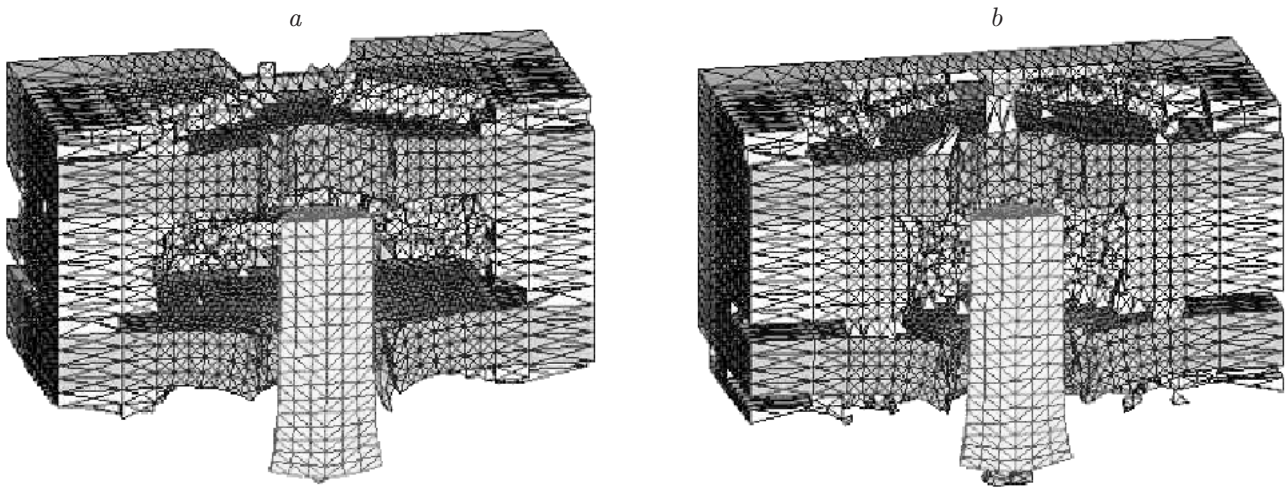

Fig. 5. Fracture in the reinforced-concrete slab: calculation by the phenomenological model (a) and by the present model (b).

to 7.65 mm) or an extended cylinder 7.65 mm in diameter and 23 mm long. The range of the impact velocities was $u_0 = 340$–750 m/sec. The parameters registered in the experiment were the projectile velocity behind the target and the diameter of spalling on the frontal and rear faces. The differences between the predicted and experimental values were 6% for the projectile velocity behind the target, 8% for the diameter of spalling on the frontal face, and 26% for the diameter of spalling on the rear face. The large difference in diameters of spalling on the rear face is caused by the difference in the target size in the computations and experiments: the maximum target size was 5.8 diameters of the projectile in the computations and 7.8 diameters of the projectile in the experiments.

Figure 2 shows the photographs of spalling on the frontal and rear faces of a reinforced-concrete slab 24 mm thick under the impact of a compact cylinder with a velocity of 462 m/sec.

Figure 3 shows the pattern of fracture of the reinforced-concrete slab under the impact of a compact projectile; this pattern was predicted by the model described above for the moment when the projectile completely ceased to move. As in the experiment, spalling is observed both on the frontal face and on the rear face. The projectile penetrated through two layers of the reinforcing net located near the frontal surface of the target and stopped when it contacted the reinforcing layers near the rear face.

Figure 4 shows the photographs of the frontal and rear surfaces of a reinforced-concrete slab 24 mm thick after impact interaction with an extended cylindrical projectile with a velocity $u_0 = 458$ m/sec.

Figure 5 shows the patterns of fracture in the reinforced-concrete slab, which were predicted by the phenomenological model and by the model described above. The differences between the phenomenological predictions and the experimental results are 6% for the projectile velocity behind the target, 3% for the diameter of spalling on the frontal face, and 26% for the diameter of spalling on the rear face, whereas the differences between the results predicted by the present model and experimental data are 4, 3, and 26%, respectively.

Conclusions. A comparison of mathematical modeling results with experimental data shows that both models can be used to calculate fracture in reinforced concrete under dynamic loading. The model proposed in the present paper is advantageous because it can be extended to calculations of strains and fracture in high-porosity types of concrete, including expanded-clay lightweight concrete. In addition, the present model allows one to study the strength of elements of reinforced-concrete structures under multiple impacts, which makes it possible to use this model for the development of engineering criteria to design earthquake-proof buildings with a reinforced-concrete frame.

This work was supported by the Russian Foundation for Basic Research (Grant No. 04-01-00856).

REFERENCES

1. N. N. Belov, D. G. Kopanitsa, O. K. Kumpyak, and N. T. Yugov, *Calculation of Reinforced-Concrete Structures under Explosive and Impact Loading* [in Russian], STT, Tomsk (2004).
2. N. N. Belov, N. T. Yugov, D. G. Kopanitsa, and A. A. Yugov, "Stress analysis of concrete and reinforced-concrete slab structures under a high-velocity impact," *J. Appl. Mech. Tech. Phys.*, **46**, No. 3, 444–451 (2005).
3. S. A. Afanas'eva, N. N. Belov, D. G. Kopanitsa, et al., "Fracture of concrete and reinforced-concrete slabs under a high-velocity impact and explosion," *Dokl. Ross. Akad. Nauk*, **401**, No. 2, 185–188 (2005).
4. N. N. Belov, V. N. Demidov, L. V. Efremova, et al., "Computed-aided modeling of high-velocity impact dynamics and associated physical phenomena," *Izv. Vyssh. Uchebn. Zaved., Fiz.*, **35**, No. 8, 5–48 (1992).
5. N. N. Belox, N. T. Yugov, D. G. Kopanitsa, and A. A. Yugov, *Impact Dynamics and Associated Physical Phenomena* [in Russian], STT, Tomsk (2005).
6. N. N. Belov, N. T. Yugov, S. A. Afanas'eva, et al., "Deformation and fracture of brittle materials," *Mekh. Kompoz. Mater. Konstr.*, **7**, No. 2, 131–142 (2001).
7. S. A. Afanas'eva, N. N. Belov, V. F. Tolkachev, et al., "Specific features of shock-wave deformation of porous ceramics Al_2O_3," *Dokl. Ross. Akad. Nauk*, **368**, No. 4, 477–479 (1999).
8. N. N. Belov, Yu. A. Biryukov, A. T. Roslyak, et al., "Mechanism of particle refinement for obtaining submicron powders of refractory compounds in a pneumatic circular machine," *Dokl. Ross. Akad. Nauk*, **397**, No. 3, 337–341 (2004).
9. L. Seaman, D. R. Curran, and D. A. Shockey, "Computational models for ductile and brittle fracture," *J. Appl. Phys.*, **47**, No. 11, 4814–4826 (1976).
10. R. L. Salganik, "Mechanics of solids with a large number of cracks," *Izv. Akad. Nauk SSSR, Mekh. Tverd. Tela*, No. 4, 149–158 (1973).
11. A. L. Isaev, "Effect of concrete reinforcement on results of dynamic loading by penetrating projectiles," in: *IIIrd Khariton's Readings*: Proc. Int. Conf. (Sarov, February 26–March 2, 2001), Inst. Exper. Phys., Sarov (2002), pp. 150–156.